A Generalized Scheme With Linear Power Balance and Uniform Switching Loss for Asymmetric Cascaded H-Bridge Multilevel Inverters

Manyuan Ye, *Member, IEEE*, Ruifan Peng, Ziwei Tong, Zihao Chen, and Zhilin Miao

***Abstract*—Under the traditional hybrid modulation strategy, the output voltage of 2:1:1 asymmetric cascaded H-bridge multilevel inverter is proved to be of high quality. However, the cascaded cells operate in unbalanced power regime and the switching loss of low-voltage cells is extremely uneven. To resolve the mentioned problems, the average power of cascaded cells is analyzed and the internal mechanism of power imbalance is revealed. Based on this, a power balance modulation strategy is proposed in this article. The modulation strategy effectively equalizes the switching loss of cells H2, H3 by modifying the triangular carriers, and then controls the conducting angle of cell H1 achieving a balanced power distribution among cascaded cells under the full modulation indexes. Compared with the existed modulation strategies, the proposed method has the merits of easy implementation, good dynamic performance, balancing low-voltage cells switching loss, and linearizing output power of cascaded cells. In addition, the modulation strategy also offers a generalized scheme, which can achieve a balanced power distribution among cascaded cells with an asymmetric ratio of i:1:1:1 …. Finally, the simulation and experiment results confirm the feasibility of the modulation strategy under changes in modulation index and load.**

***Index Terms*—Asymmetric multilevel inverter, balanced switching loss, carrier rotation, hybrid modulation strategy, linear power balance.**

I. Introduction

RECENTLY, with the boosting development of power electronics, multilevel inverters based on pulsewidth modulation (PWM) strategy have become a competitive solution for medium-voltage drive systems [1]. Multilevel inverters have been employed in numerous applications for excellent harmonic performance, high efficiency, low dv/dt, easy modularization [2], [3], such as electric vehicle, high-voltage direct current (HVDC) transmission, grid-connected photovoltaic energy conversion systems, active power filtering (APF), etc. [4], [5].

According to the topology of multilevel inverters, they are mainly classified into three categories: such as neutral point clamped, flying capacitor, and cascaded H-bridge (CHB) [6], [7]. Compared with the other topologies, though CHB multilevel inverters acquire multiple dc sources, they do not need to handle the problem of voltage balancing among dc-link capacitors, which reduces the complexity of the control system a lot [8], [9].

CHB multilevel inverters can be divided into two groups: symmetric CHB multilevel inverters (SCHBMLIs) and asymmetric CHB multilevel inverters (ACHBMLIs), according to the amplitudes of dc source of the cascaded cells [10], [11]. If the amplitudes are equal, they are classified as SCHBMLIs. and if the amplitudes are unequal, they are denoted ACHBMLIs. Compared with the SCHBMLIs, ACHBMLIs can acquire a higher number of levels of the output voltage without increasing the number of switches and dc sources [12]. The topology of multilevel inverters and modulation strategy are auxiliary to each other, and they jointly determine the quality of the output voltage. ACHBMLIs often adopt the hybrid modulation strategy, where several cascaded cells generate stepped waveform and the PWM modulation is employed to other cells. However, if the hybrid modulation strategy is not proper, the problem of current reverse among cascaded cells may occur in ACHBMLIs, which would boost the dc-link capacitor voltage and affect the quality of output voltage.

To eliminate the drawbacks of current reverse among ACHBMLIs, a modified hybrid modulation strategy for the ACHBMLIs with an asymmetric ratio of 2:1 is proposed in [13], which enables the output voltage polarity of the cascaded cells to keep the same. And the switches utilization among a module is uniform under the modulation strategy. Nevertheless, the modulation strategy is hard to implement: the modulation signal is modified in five intervals and the signals of switches are need to be converted by complex programmable logic devices. The modulation strategy in [14] realizes the continuous PWM modulation under the full modulation indexes. At the same time, the problem of current reverse among cascaded cells is avoided under the modulation strategy. But the switching loss of the low-voltage cells is extremely uneven and the cascaded cells operate in unbalanced power regime, which will result in nonuniform utilization of dc sources and distortion in input current.

Manuscript received April 11, 2021; revised August 13, 2021; accepted September 16, 2021. Date of publication September 21, 2021; date of current version November 30, 2021. This work was supported in part by the National Natural Science Foundation of China, in part by Key R&D Projects in Jiangxi Province, and in part by Graduate Innovation Foundation of Jiangxi Province under Grant 51767007, Grant 20202BBEL53034, Grant 20192BBEL50011, and Grant YC2020-S307. Recommended for publication by Associate Editor P. Barbosa. (*Corresponding author: Manyuan Ye*.)

The authors are with the School of Electrical and Automation Engineering, East China Jiaotong University, Nanchang 330013, China (e-mail: yemanyuan1@163.com; 1652563539@qq.com; 690444970@qq.com; 1343085939@qq.com; 798539149@qq.com).

Color versions of one or more figures in this article are available at https://doi.org/10.1109/TPEL.2021.3114369.

Digital Object Identifier 10.1109/TPEL.2021.3114369

Apart from avoiding the current reverse, achieving a balanced power distribution among cascaded cells of multilevel inverters is also a key factor. The carriers are modified in [15], which achieves a balanced power distribution among the submodules and reduces the voltage ripple of capacitors. Whereas, the method generates larger common-mode voltage and higher total harmonic distortion (THD) of the output voltage. Not only an even power distribution among cascaded cells is achieved in [16], but also the switches utilization is uniform. However, the scheme increases the switching loss of devices and the efficiency of the inverter is decreased. A single-carrier-based PWM scheme is proposed in [17], which reduces the number of the carrier signals and maintains a nearly equal distribution of the overall real power among the cascaded cells.

The mentioned modulation strategies in [15]–[17] can achieve equal power outputs among cascaded cells of SCHBMLIs, but they are not suitable for ACHBMLIs. A transformer-based asymmetric multilevel inverter with only a dc source is used in [18], whose asymmetric ratio is 6:7:8:9 produced by changing the transformers' turn ratio. The inverter can synthesize an output voltage of 35 levels and achieve balanced power distribution among the cascaded stages by reproducing the selected switching patterns. But the switching patterns are calculated offline and some cascaded cells would feed power into other cells. A modified hybrid modulation strategy for 2:1 ACHBMLIs is proposed in [19]. Under the modulation strategy, the problem of current reverse is settled and the power balance among cascaded cells is achieved. Based on the method of [19], the modulation strategy of 2:1:1 ACHBMLIs is investigated in [20]. Phase shift PWM (PS-PWM) and phase disposition PWM (PD-PWM) modulation are employed to two low-voltage cells and the conducting angle of cell H1 is modified, which achieves a balanced power distribution among cascaded cells. Nevertheless, the mentioned schemes in [18]–[20] are designed for specific ACHBMLIs and they cannot be extended to apply in other ACHBMLIs.

The rest of this article is organized as followed. The inverter studied in this article is completely described in Section II. Section III illustrates the improved hybrid modulation strategy and the power distribution among cascaded cells is presented in Section IV. The principle of the power balance method of IH-PWM and the switching loss of cells H2, H3 under the PBIH-PWM are depicted in Section V. To illustrate the merits of the proposed modulation strategy, the comparison results with other schemes are given in Section VI. Simulation results in Section VII and experiment results in Section VIII verify the feasibility of the modulation strategy under step change in modulation index and sudden load change. And a generalized scheme based on the PBIH-PWM is represented in the Appendix, which can achieve a balanced power distribution among cascaded cells of ACHBMLIs with an asymmetric ratio i:1:1:1 . . . . .

II. Circuit Configuration of Asymmetric Cascaded Nine-Level Inverter

The schematic diagram of asymmetric cascaded nine-level inverter studied in this article is shown in Fig. 1. As can be observed, the inverter is composed of three CHB cells with an asymmetric ratio of 2:1:1. And u_{H1}, u_{H2}, and u_{H3} are the instantaneous output voltage of cells H1, H2, and H3, respectively. For the cascaded cells connected in series, the inverter output voltage u_{AN} can be calculated as follows:

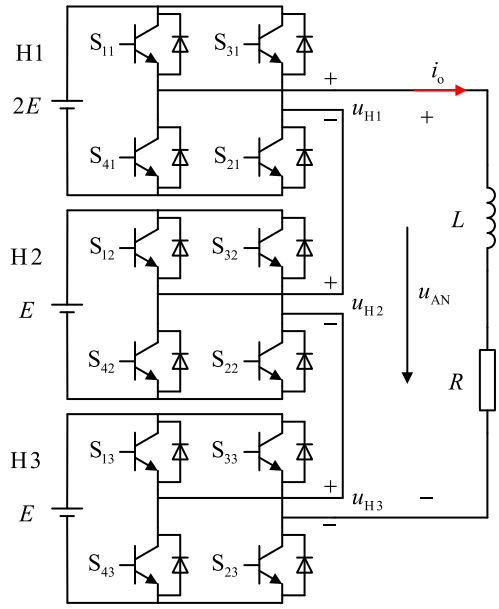

Fig. 1. Asymmetric cascaded nine-level inverter topology.

$$u_{\mathrm{AN}} = u_{\mathrm{H1}} + u_{\mathrm{H2}} + u_{\mathrm{H3}}. \tag{1}$$

Considering that the resistance-inductance load is connected to the inverter output, the inverter output current i_{o} can be defined as by ignoring the existence of harmonics

$$i_{\mathrm{o}} = I\sin(\omega t + \arctan(\omega L/R)) \tag{2}$$

where I is the amplitude of the inverter output current i_{o}. S_i is defined as the switching state of the cells Hi(i = 1,2,3).

And when the corresponding device S_{mi}(m = 1,2,3,4) is on, S_{mi} takes the value:1, or the value of S_{mi} is 0.

$$S_i = \mathrm{S}1_i\mathrm{S}2_i - \mathrm{S}3_i\mathrm{S}4_i. \tag{3}$$

Thus, S_i takes three values: 1, 0, −1 and the corresponding cell Hi output voltage has three levels. So, the inverter could obtain a signal with nine levels by synthesizing the output voltage of cascaded cells: $\pm 4E$, $\pm 3E$, $\pm 2E$, $\pm E$, and 0. Then, (1) can be rewritten as follows:

$$u_{\mathrm{AN}} = S_1 \cdot 2E + (S_2 + S_3) \cdot E. \tag{4}$$

As can be observed from (3) and (4), there are 27 combinations of switching states to synthesis the inverter output voltage u_{AN}. So, some levels of signal u_{AN} can be synthesized by multiple switching states. However, under some combination states, the output voltage polarities of cascaded cells are opposite, which would cause current reverse and boost the voltage of dc-link capacitor. In order to resolve the problem effectively, only the combination states are remained which ensures the polarities of the cascaded cells output voltage are same. After screening, the

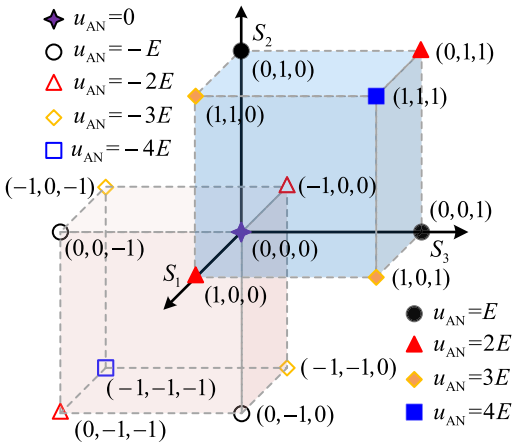

Fig. 2. Relationship between output phase voltage of the inverter and switching states.

remained switching states used to synthesize the inverter output voltage u_{AN} are depicted in Fig. 2.

III. Improved Hybrid Modulation Strategy

Based on the traditional hybrid modulation strategy, an improved hybrid modulation PWM (IH-PWM) strategy is proposed in this article. The staircase modulation is applied to cell H1, which could effectively reduce the switching loss. And there are two choices for the cells H2, H3:PS-PWM and PD-PWM. When the modulation index and equivalent switching frequency of devices are same, under PS-PWM strategy, the power distribution among cascaded cells and loss of devices are even. However, when the PS-PWM strategy is applied to three-phase inverters, the level jumping would occur in line voltage, which is unfavorable for industrial applications; Under PD-PWM strategy, the quality of line voltage is better, and the THD of line voltage is smaller. Although the losses and switching stress of devices are different, these drawbacks can be overcome by carrier rotation. So, the PD-PWM strategy is applied to the cells H2, H3.

The principle of IH-PWM strategy is shown in Fig. 3, which could effectively resolve the problem of current reverse. v_m is the modulation signal of cell H1 and v_{cr1}, v_{cr1-} are carriers of cell H1. As shown in Fig. 3, when $v_m > v_{cr1}$ during the positive half-cycle or $v_m < v_{cr1-}$ in the negative half-cycle, cell H1 begins to output square waveform. The modulation signal v'_m of cells H2, H3 is obtained by subtracting the output voltage of cell H1 u_{H1} from the modulation signal v_m. When v'_m is bigger than v_{cr2} during the positive half-cycle or v'_m is smaller than v_{cr2-} in the negative cycle, cell H2 begins to work and generates a PWM waveform. The modulation principle of cell H3 is similar to that of cell H2, so it will not be repeated here.

IV. Analysis of the IH-PWM Strategy Output Power

Assuming that the modulation signal v_m is

$$v_m = A_m \sin \omega t \tag{5}$$

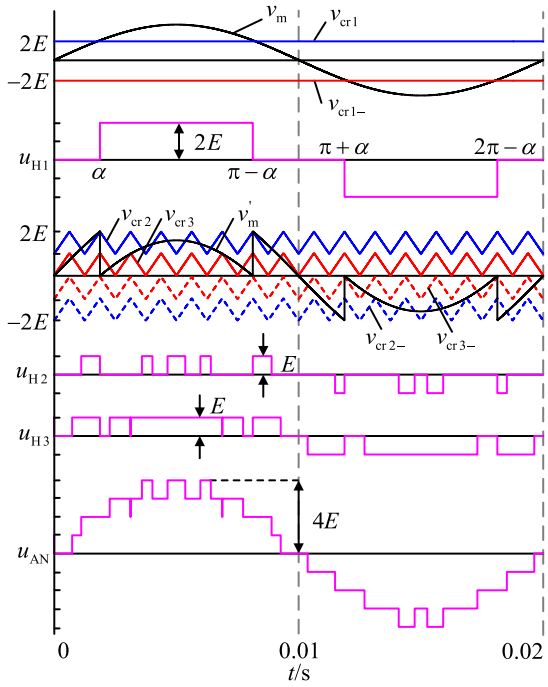

Fig. 3. Modulation principle of the IH-PWM.

where A_m is the amplitude of v_m. The modulation index m_a generally is defined as $m_a = A_m/8\,A_{cr}$, where A_{cr} is the amplitude of carriers. And α_i is the conducting angle, which can be expressed as follows:

$$\alpha_i = \arcsin \frac{i}{4m_a} (i = 1, 2, 3). \tag{6}$$

According to the principle of the IH-PWM strategy, the output voltage of cell H1 u_{H1} can be expressed as (7), which is defined from the Fourier series expansion. Similarly, the output voltage v_o superposed by cell H2 and cell H3 can be expressed as follows:

$$u_{H1} = \begin{cases} 0 m_a \in (0, 0.5) \\ \sum\limits_{k=1,3,5\cdots}^{\infty} \frac{8E}{k\pi} \cos(k\alpha_2) \sin(k\omega t) m_a \in (0.5, 1) \end{cases} \tag{7}$$

$$v_o = \begin{cases} 4m_a E \sin(\omega t) m_a \in (0, 0.5) \\ \sum\limits_{k=1,3,5\cdots}^{\infty} [\frac{4E(km_a\pi - 2\cos(k\alpha_2))}{k\pi}] \sin(k\omega t) \\ m_a \in (0.5, 1) \end{cases}. \tag{8}$$

For the cascaded multilevel inverter, the average power of the cascaded cells can be computed as follows:

$$P_{Hi} = \frac{1}{T} \int_0^T u_{Hi} i_o dt = 0.5 u_{Hi(1)} I \cos \varphi \tag{9}$$

where $u_{Hi(1)} (i = 1,2,3)$ is the amplitude of fundamental component of the cascaded cells, and φ is the phase shift among the fundamental component and the inverter output current. Combining (7)–(9) and according to the principle of IH-PWM strategy, the average power of the cascaded cells can be expressed as follows:

$$P_{H1} = \begin{cases} 0 & m_a \in (0, 0.5) \\ \frac{4EI\cos\varphi}{\pi} \sqrt{1 - \frac{1}{4m_a^2}} & m_a \in (0.5, 1) \end{cases} \tag{10}$$

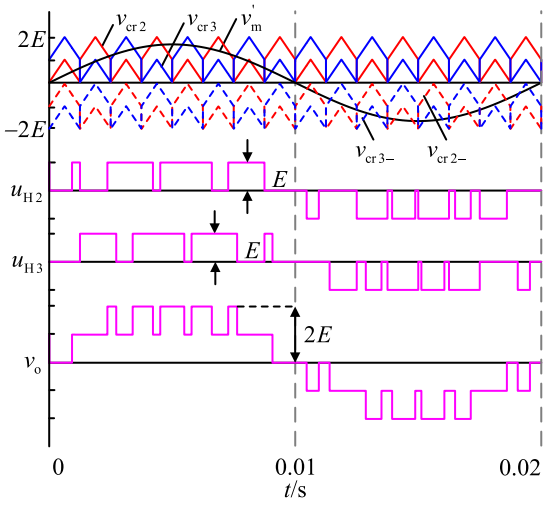

Fig. 4. Principle of modified IPD strategy.

$$P_{H2}=\begin{cases}0 m_a\in(0,0.25)\\ \frac{2EI\cos\varphi}{\pi}[2m_a(\frac{\pi}{2}-\alpha_1+\frac{1}{2}\sin 2\alpha_1)-\cos\alpha_1]\\ m_a\in(0.25,0.5)\\ \frac{2EI\cos\varphi}{\pi}[2m_a(\frac{1}{2}\sin 2\alpha_1-\frac{1}{2}\sin 2\alpha_2+\alpha_2-\\ \alpha_1)-\cos\alpha_1+\cos\alpha_2]\\ m_a\in(0.5,0.75)\\ \frac{2EI\cos\varphi}{\pi}[2m_a(\frac{\pi}{2}+\alpha_2-\alpha_1-\alpha_3+\frac{1}{2}\sin 2\alpha_1\\ +\frac{1}{2}\sin 2\alpha_3-\frac{1}{2}\sin 2\alpha_2)-3\cos\alpha_3+\cos\alpha_2-\\ \cos\alpha_1]m_a\in(0.75,1)\end{cases} \tag{11}$$

$$P_{H3}=\begin{cases}2m_aEI\cos\varphi m_a\in(0,0.25)\\ \frac{2EI\cos\varphi}{\pi}[2m_a(\alpha_1-\frac{1}{2}\sin 2\alpha_1)+\cos\alpha_1]\\ m_a\in(0.25,0.5)\\ \frac{2EI\cos\varphi}{\pi}[2m_a(\frac{\pi}{2}+\alpha_1-\alpha_2+\frac{1}{2}\sin 2\alpha_2-\\ \frac{1}{2}\sin 2\alpha_1)+\cos\alpha_1-3\cos\alpha_2]\\ m_a\in(0.5,0.75)\\ \frac{2EI\cos\varphi}{\pi}[2m_a(\alpha_1+\alpha_3-\alpha_2+\frac{1}{2}\sin 2\alpha_2-\\ \frac{1}{2}\sin 2\alpha_1-\frac{1}{2}\sin 2\alpha_3)+\cos\alpha_1-3\cos\alpha_2+\\ 3\cos\alpha_3]m_a\in(0.75,1)\end{cases} \tag{12}$$

V. 2:1:1 Linear Power Balance Method of the IH-PWM

To resolve the problem of unbalanced power distribution among cascaded cells, a power balance improved hybrid modulation PWM (PBIH-PWM) strategy is proposed. The principle of the strategy is illustrated in Fig. 4. As can be observed, the carriers of cells H2, H3 are modified to achieve a balanced power distribution among cells H2, H3: v_{cr2}, v_{cr3-} are rotated by adding a square waveform with half the frequency of the carriers; v_{cr3}, v_{cr2-} are modified by subtracting a square waveform with half the frequency of the carriers.

To illustrate why the power balance can be achieved under the strategy, the output voltage v_o superposed by cells H2, H3 during the positive half-cycle is analyzed, which is depicted in Fig. 5. In Fig. 5, T_c is the carrier cycle, and v_{cr2} and v_{cr3} are

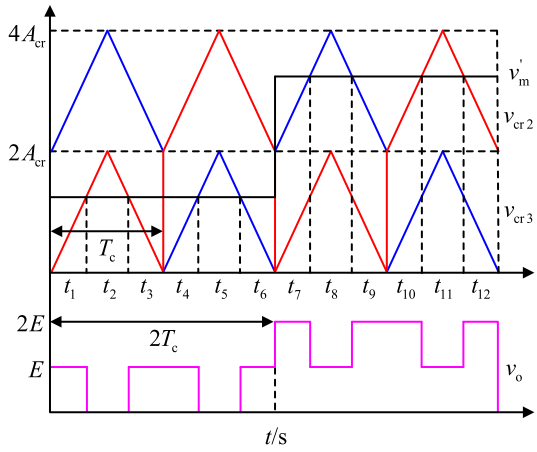

Fig. 5. Geometric relationship between the triangle carriers and the modulation wave.

the carriers of cells H2, H3, respectively. Assuming the A_{m1} is the amplitude of the modulation signal v'_m. And m_{a1} is defined as the modulation index of cells H2, H3, which is expressed as follows:

$$m_{a1}=A_{m1}/(4A_{cr}). \tag{13}$$

Since the frequency of carrier f_{cr} is much larger than the frequency of modulation wave f_m, the instantaneous value of modulation signal v'_m can be regarded as constant in the relevant carrier cycles. When the instantaneous value of v'_m is $0\le v'_m \le 2A_{cr}$, the average output voltage of cells H2, H3 in the two carrier cycles is

$$\bar{u}_{H2(2T_c)}=\frac{t_1+t_3}{2T_c}v'_m=\frac{8m_{a1}E\sin(2\pi f_m t)}{f_{cr}}=0.5\bar{v}_{o(2T_c)} \tag{14}$$

$$\bar{u}_{H3(2T_c)}=\frac{t_4+t_6}{2T_c}v'_m=\frac{8m_{a1}E\sin(2\pi f_m t)}{f_{cr}}=0.5\bar{v}_{o(2T_c)}. \tag{15}$$

Similarly, when the instantaneous value of v'_m is $0\le v'_m \le 2A_{cr}$, the average output voltage of cells H2, H3 in the two carrier cycles is

$$\bar{u}_{H2(2T_c)}=\frac{T_c+t_{10}+t_{12}}{2T_c}v'_m=\frac{8m_{a1}E\sin(2\pi f_m t')}{f_{cr}}=0.5\bar{v}_{o(2T_c)} \tag{16}$$

$$\bar{u}_{H3(2T_c)}=\frac{T_c+t_7+t_9}{2T_c}v'_m=\frac{8m_{a1}E\sin(2\pi f_m t')}{f_{cr}}=0.5\bar{v}_{o(2T_c)}. \tag{17}$$

Regardless of the loss of the diodes, which is parallel to the switches, the loss of cascaded cells can be classified into switching loss and conduction losses. Under the PBIH-PWM strategy, the switching frequency of cascaded cells and the ratio of the conduction time of devices are same, so the switching loss

TABLE I
SWITCHING LOSS OF CELLS H2, H3 UNDER DIFFERENT MODULATION INDEXES

Modulation index (m_a)	0.1	0.2	0.3	0.4	0.5	0.6	0.7	0.8	0.9	1
I/A	1.187	2.113	3.124	4.173	4.992	6.175	7.102	8.111	9.162	9.990
Cell H2 devices switching times	245	244	244	244	238	228	214	213	210	214
Cell H3 devices switching times	244	244	243	244	238	228	214	212	210	214
Switching loss of cell H2 /W	5.48	7.22	9.39	11.12	12.68	13.95	14.66	16.26	17.75	19.93
Switching loss of cell H3 /W	5.46	7.22	9.35	11.12	12.68	13.95	14.66	16.18	17.75	19.93

of cells H2, H3 can be expressed as follows:

$$P_{\mathrm{SS(H2)}} = P_{\mathrm{SS(H3)}} = \frac{4}{\pi}\sum_{n=1}^{f_{\mathrm{sw}}}(E_{\mathrm{sw(on)}}+E_{\mathrm{sw(off)}}) \tag{18}$$

where f_{sw} is the switching frequency of devices, and $E_{\mathrm{sw(on)}}$, $E_{\mathrm{sw(off)}}$ is the energy loss of the device turn-on and turn-off, respectively.

To evaluate the switching loss of cells H2, H3, the asymmetric cascaded nine-level inverter with the dc source voltage $E =$ 50 V at the frequency of carrier $f_{\mathrm{cr}} = 8$ kHz is tested. An *R-L* load(20 Ω, 4 mH) is connected to the inverter output. And taking SGH40N60 as the switches, the switches are also used in the subsequent experiment. According to the datasheet of the switches in [21] and the mathematical models in [22], the switching loss of cells H2, H3 are calculated. Table I shows the switching loss of cells H2, H3 under different modulation indexes. As it can be observed, the switching loss of cells H2, H3 always keep consistent under different modulation indexes.

And the ratio of the conduction time of cells H2, H3 is

$$\tau_{\mathrm{H2}} = \tau_{\mathrm{H3}} = m_{\mathrm{a1}}\sin(2\pi f_{\mathrm{cr}}t) - 0.5 \tag{19}$$

The conduction loss of cells H2, H3 can be expressed as follows:

$$P_{\mathrm{CON(H2)}} = P_{\mathrm{CON(H3)}} = \frac{2}{\pi}\int_0^{\pi}(u_{\mathrm{on}}(t) * i_{\mathrm{o}}(t)\tau(t)dt. \tag{20}$$

Substituting (2), (19) into (20), the conduction loss of cells H2, H3 can be rewritten as follows:

$$P_{\mathrm{CON(H2)}} = P_{\mathrm{CON(H3)}} = m_{\mathrm{a1}}v_{CE0}I\cos\varphi - I^2 r_{CE}\left(\frac{8}{3\pi}m_{\mathrm{a1}}\cos^2\varphi - \frac{1}{2}\right) \tag{21}$$

where v_{CE0} is the voltage between the collecting electrode and the emitter electrode when the IGBT of cascaded cells is on, and r_{CE} is the equivalent resistance.

As it can be noted from the previous analysis, balanced switching loss and power distribution among cells H2, H3 are achieved under the modified IPD strategy.

To achieve a balanced power distribution among the three cascaded cells, the conducting angle of cell H1 is modified and the fundamental amplitude of cell H1 output voltage $u_{\mathrm{H1(1)}}$ is half of the fundamental amplitude of the inverter output voltage $u_{\mathrm{AN(1)}}$, which can be calculated as follows:

$$u_{\mathrm{H1(1)}} = \frac{8E}{\pi}\cos\left(\mathrm{acos}\left(\frac{\pi m_{\mathrm{a}}}{4}\right)\right) = 2m_{\mathrm{a}}E \tag{22}$$

and the fundamental amplitudes of cells H2, H3 output voltage $u_{\mathrm{H2(1)}}$, $u_{\mathrm{H3(1)}}$ are

$$u_{\mathrm{H2(1)}} = u_{\mathrm{H3(1)}} = \frac{1}{2}v_{\mathrm{o(1)}} = \frac{1}{2}(4m_{\mathrm{a}}E - u_{\mathrm{H1(1)}}) = m_{\mathrm{a}}E. \tag{23}$$

Hence, the average output power of the three cascaded cells is

$$P_{\mathrm{H1}} = m_{\mathrm{a}}EI\cos\varphi, P_{\mathrm{H2}} = P_{\mathrm{H3}} = \frac{1}{2}m_{\mathrm{a}}EI\cos\varphi. \tag{24}$$

The PBIH-PWM strategy can achieve P_{H1}:P_{H2}:$P_{\mathrm{H3}} = 2$:1:1 under the full modulation indexes, so the power balance of three cascaded cells is realized.

VI. COMPARISON WITH OTHER MODULATION STRATEGIES

The PBIH-PWM strategy is compared with the other modulation strategies [13]–[18], [20]. The modulation strategies [15]–[17] can distribute power evenly among the cascaded cells. However, they are only suitable for SCHBMLIs and the comparison results are not depicted in Table II. The modulation strategy in [13] and [14] is hard to implement: the modulation signal is modified 5 times in different intervals and the signals of switching devices are converted by 15 times logical operations [13]; the modulation signal is modified 2 times and the signals of switching devices are superposed 2 times [14]; Besides, the cascaded cells operate in unbalanced power regime. And the method proposed in [18] can achieve a balanced power distribution among cascaded cells, but the output power of cascaded cells increases nonlinearly and the maximum deviation of the balanced power distribution is 10%. The scheme in [20] achieves a balanced power distribution among cascaded cells, but THD of u_{AN} is higher than that under PBIH-PWM because PS+PD PWM modulation is applied to cells H2, H3.

The relationships between the average output power of cascaded cells and modulation index under different modulation strategies are presented in Fig. 6. As it is noted, the output power of cascaded cells is unbalanced in [13], and only the average output power of cell H2 increases linearly from 0 to 0.1625 *EI*cosφ

TABLE II
COMPARISON OF DIFFERENT MODULATION STRATEGIES FOR ACHBMLIS

	The range of power linearization	Modulation strategy	Power balance	Cells H2, H3 switching loss equalization
[13]	H1: NO H2: $m_a \in (0\sim0.325)$	H1: IPD + logical operation H2:IPD	Unable power balance	/
[14]	H1: NO H2: $m_a \in (0\sim0.25)$ H3: NO	H1, H2: staircase modulation H3:IPD	Unable power balance	NO
[18]	NO	Off-line calculation of switching patterns	Nonlinear power balance	/
[20]	H1: $m_a \in (0\sim1)$ H2: $m_a \in (0\sim1)$ H3: $m_a \in (0\sim1)$	H1: staircase modulation H2, H3: PS+PD	Linear power balance	YES
IH-PWM	H1: NO H2: NO H3: $m_a \in (0\sim0.25)$	H1: staircase modulation H2, H3: IPD	Unable power balance	NO
PBIH-PWM	H1: $m_a \in (0\sim1)$ H2: $m_a \in (0\sim1)$ H3: $m_a \in (0\sim1)$	H1: staircase modulation H2, H3: modified IPD	Linear power balance	YES

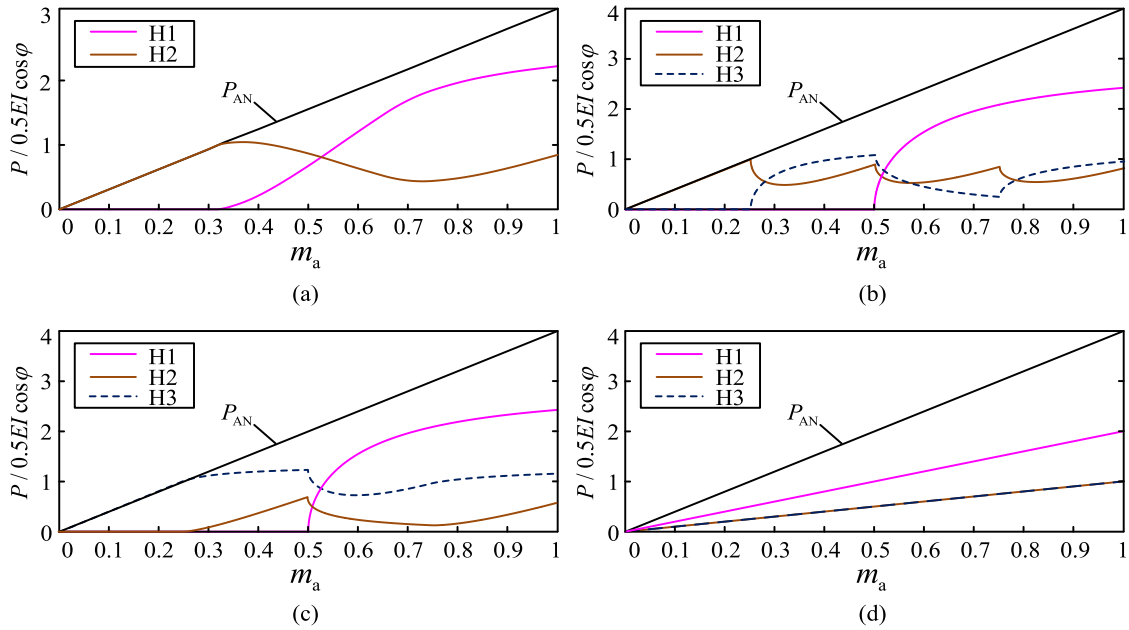

Fig. 6. Relationship between the cascaded cells' average output power and modulation index under different modulation strategies. (a) Literature [13]. (b) Literature [14]. (c) IH-PWM. (d) PBIH-PWM.

when m_a varying from 0 to 0.325. The average output power of cell H2 [14] and cell H3 (IH-PWM) increase linearly from 0 to 0.5 $EI\cos\varphi$, respectively, when m_a varying from 0 to 0.25. And under the PBIH-PWM strategy, the average output power of cells H1, H2, H3 increases linearly under the full modulation indexes. In addition, a balanced power distribution among cascaded cells is achieved under the full modulation indexes.

VII. SIMULATION RESULTS

An asymmetric cascaded nine-level inverter model is built in MATLAB/Simulink environment to verify the correctness of the proposed modulation strategy. The results are obtained with different modulation indexes under both the IH-PWM and PBIH-PWM strategies. The model parameters are listed in Table III.

TABLE III
PARAMETERS OF SIMULATION MODEL

Simulation parameters	Values
DC source voltage of cell H1	100V
DC source voltage of cells H2, H3	50V
Frequency of modulation wave f_m	50Hz
Frequency of carrier f_{cr}	8kHz
Modulation index m_a	0.35, 0.65, 0.95

The results obtained under the IH-PWM strategy and the PBIH-PWM strategy at $m_a = 0.35, 0.65, 0.95$ are depicted in Fig. 7(a) and (b), respectively. As it can be noted, under the

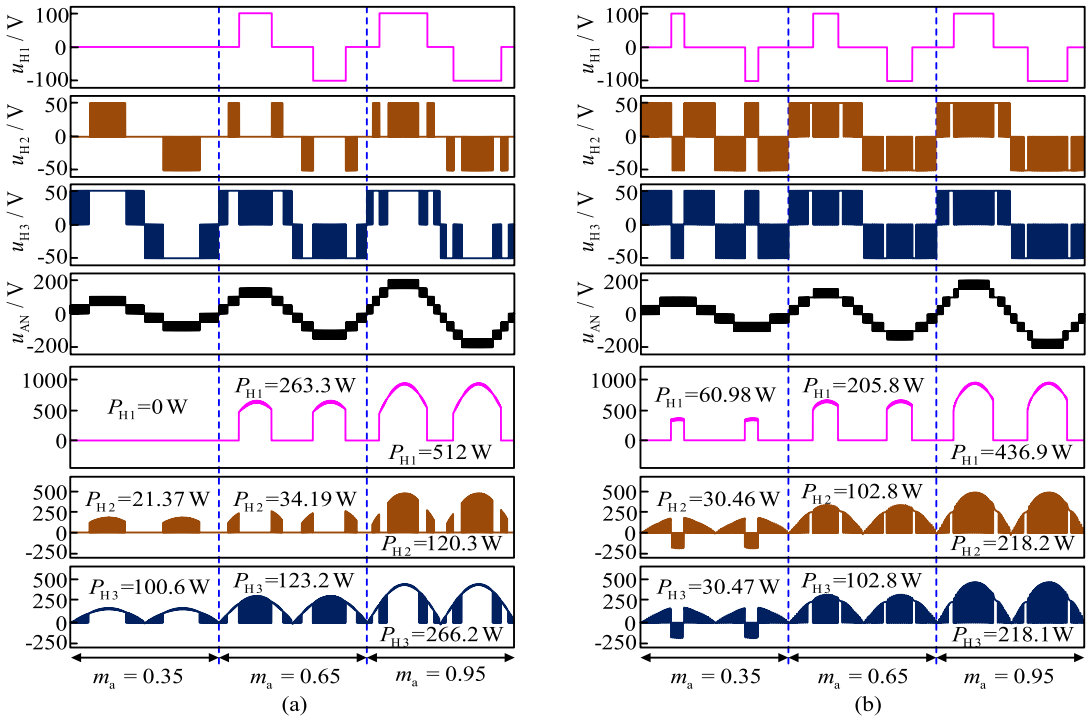

Fig. 7. Simulation results under IH-PWM and PBIH-PWM. (a) Output voltage waveforms and average power waveforms of cascaded cells under IH-PWM strategy. (b) Output voltage waveforms and average power waveforms of cascaded cells under PBIH-PWM strategy.

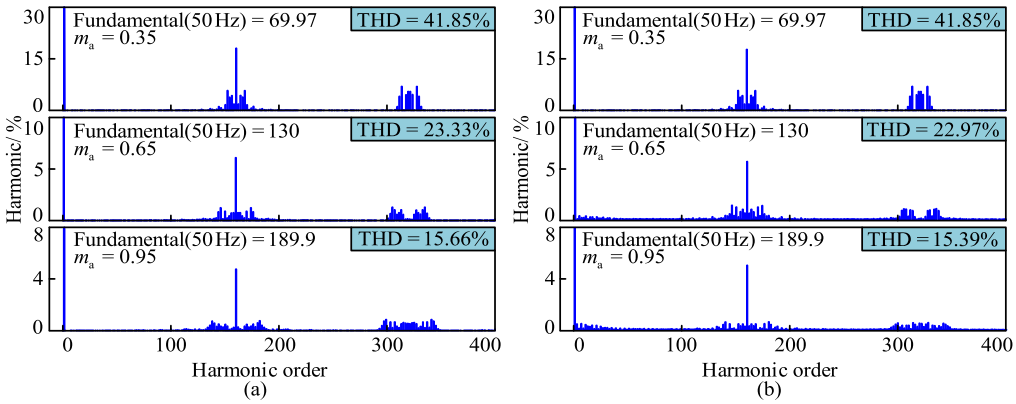

Fig. 8. Spectra of the inverter output voltage uAN under IH-PWM and PBIH-PWM at different modulation indexes. (a) FFT results under IH-PWM strategy. (b) FFT results under PBIH-PWM strategy.

IH-PWM strategy, cell H1 does not participate in synthesizing the output voltage when m_a at 0.35. And cell H1 generates a square waveform when m_a at 0.65, 0.95. The output voltage waveforms of cells H2, H3 are quite different, but they are all PWM waves of three levels at different modulation indexes. And the average output power of cell H1 is zero. Under the IH-PWM, the average output power of cell H3 is always bigger than the counterpart of cell H2 at different modulation indexes. The ratio of the average output power of three cascaded cells does not meet the 2:1:1 linear balance condition. In other words, the cascaded cells operate in unbalanced power regime. Under the PBIH-PWM strategy, cell H1 always participates in synthesizing the output voltage at different modulation indexes. And the output voltage waveforms of cells H2, H3 are similar. It can be seen from Fig. 7(b), the average output power of cascaded cells presents the 2:1:1 linear relationship at different modulation indexes, so the power balance among cascaded cells is achieved. Furthermore, Fig. 7(b) shows the waveforms of the output voltage and the output power of cascaded cells under a change in modulation index m_a from 0.35 to 0.65, then to 0.95. As it can be noted, the inverter output voltage u_{AN} varies from a PWM wave of 5-level to 7-level, then to 9-level. And the PBIH-PWM can achieve a balanced power distribution among cascaded cells despite modulation index changes.

The FFT results of u_{AN} under IH-PWM and PBIH-PWM at different modulation indexes are shown in Fig. 8. It can be

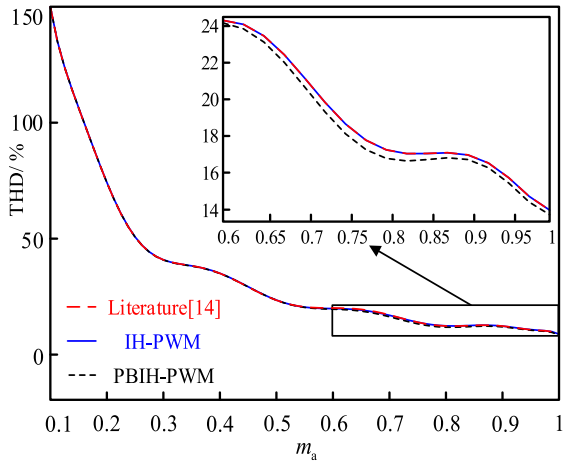

Fig. 9. THD of inverter output voltage under different modulation strategies.

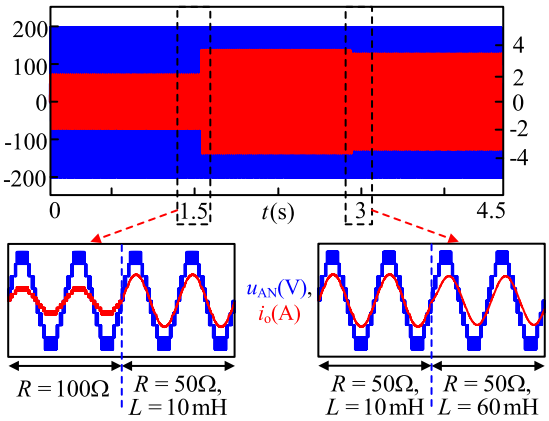

Fig. 10. Simulation results of output voltage, inverter output current with changes in load.

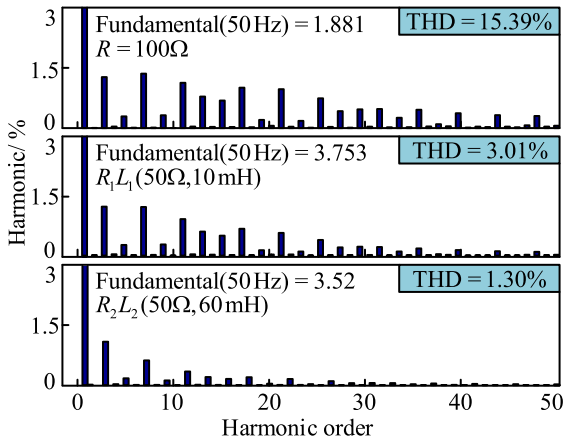

Fig. 11. Spectra of inverter output current with changes in load.

seen that the main harmonics for both are concentrated around 8 kHz. And the values of the THD of u_{AN} are all 41.85% at m_a = 0.35 under the IH-PWM and PBIH-PWM. But the value of the THD of u_{AN} under PBIH-PWM is 0.3% smaller than that under IH-PWM at m_a = 0.65,0.95. However, the amplitudes of

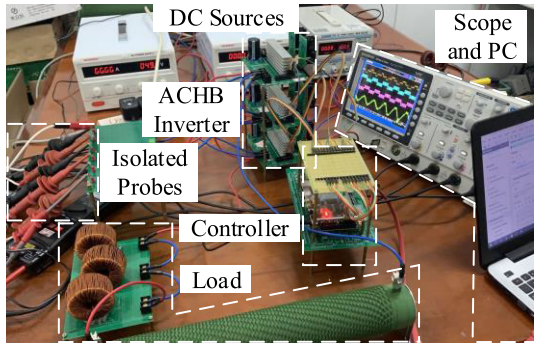

Fig. 12. Photograph of the experimental protype.

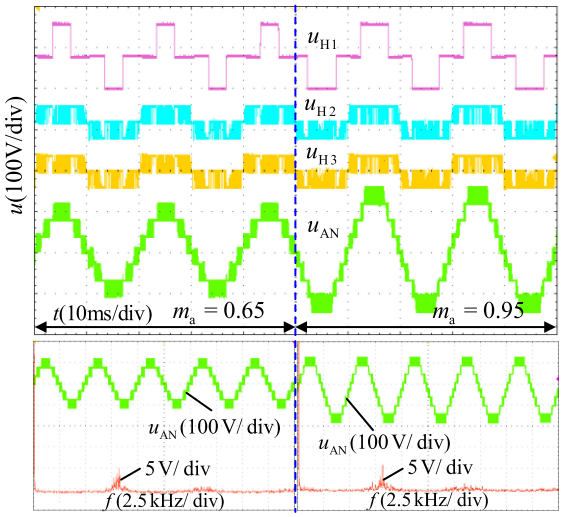

Fig. 13. Experiment results under PBIH-PWM with changes in modulation index.

the fundamental voltage of u_{AN} are same at m_a = 0.35,0.65,0.95 under IH-PWM and PBIH-PWM. And the variations in the THD of u_{AN} with modulation index m_a are depicted in Fig. 9 under different modulation strategies. As it is noted, when modulation index m_a varying from 0 to 0.6, the THD under different modulation strategies is almost same. For ma larger than 0.6, the output voltage THD of IH-PWM and the modulation strategy in [14] are same and larger than PBIH-PWM. Therefore, PBIH-PWM can improve the quality of the output voltage slightly.

Fig. 10 depicts the waveforms of asymmetric cascaded nine-level inverter with the changes of the load from R (100 Ω) to R_1L_1(50 Ω-10 mH, PF = 0.99, at t = 1.5 s), then to R_2L_2(50 Ω-10 mH, PF = 0.99, at t = 3 s) when the modulation index is set to 0.95. As it can be observed, the output voltage u_{AN} of the inverter is maintained at a 9-level PWM wave and the amplitude of u_{AN} is 200 V under sudden load change. The amplitude of the inverter output current i_o changes from 2 to 3.838 A and finally to 3.568 A. In addition, i_o can be made more sinusoidal-like for larger inductance. It can be seen from Fig. 11 that the THD of i_o decreases from 15.39% to 3.01%, then to 1.30% when the load changes. And the maximum single harmonic of i_o is below 1.41% with an R-L load. The results indicate the PBIH-PWM strategy has good dynamic performance.

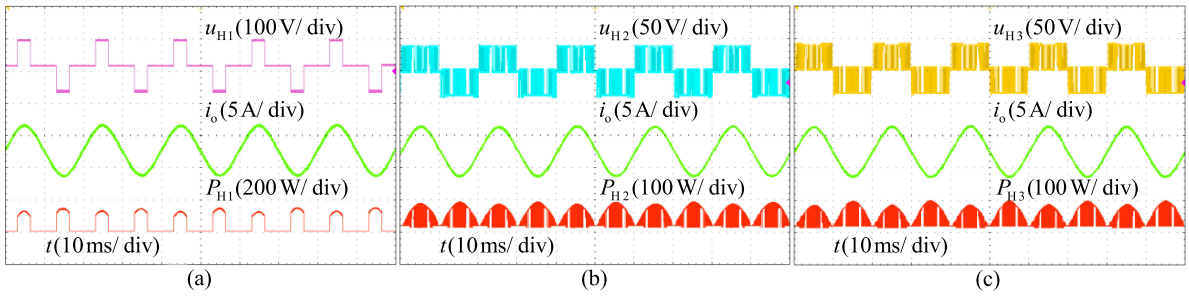

Fig. 14. Experiment results of average power of cascaded cells with modulation index is 0.65. (a) Average power of cell H1. (b) Average power of cell H2. (c) Average power of cell H3.

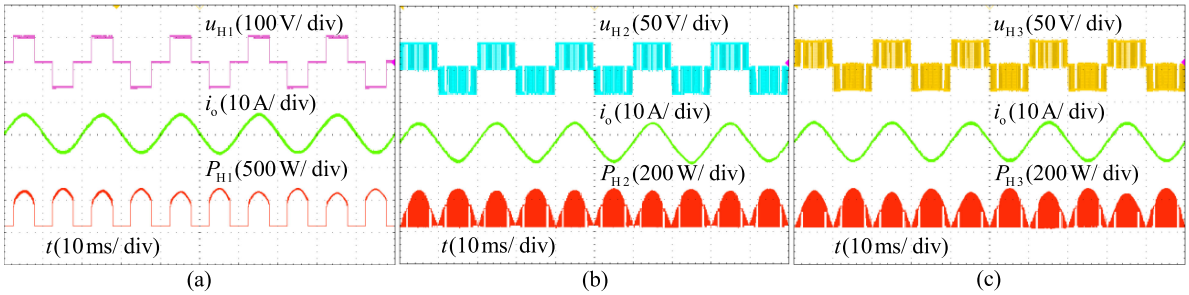

Fig. 15. Experiment results of average power of cascaded cells with modulation index is 0.95. (a) Average power of cell H1. (b) Average power of cell H2. (c) Average power of cell H3.

TABLE IV
PARAMETERS OF EXPERIMENTAL PROTOTYPE

Experimental parameters	Values
DC source voltage of cell H1	80V
DC source voltage of cells H2, H3	40V
Frequency of modulation wave f_m	50Hz
Frequency of carrier f_{cr}	8kHz
Modulation index m_a	0.65, 0.95

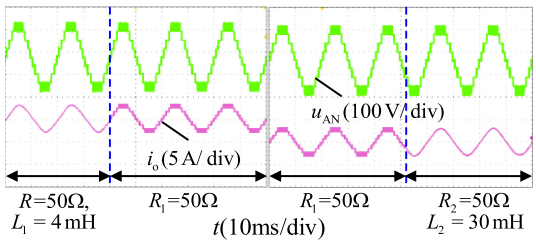

Fig. 16. Experiment results of uAN, io with changes in load.

VIII. EXPERIMENT

Because the scheme is difficult to implement using a DSP chip. The experimental prototype shown in Fig. 12 is designed to validate the feasibility of the proposed PBIH-PWM strategy, whose controller is based on the DSP TMS320F28335 chip and the FPGA ZYNQ7010 chip. The parameters of the experimental prototype are shown in Table IV.

The experiment results under PBIH-PWM are shown in Fig. 13 when modulation index m_a changes from 0.65 to 0.95. As can be seen, the cell H1 the inverter output voltage u_{AN} changes from a 7-level PWM wave to 9-level when modulation index changes from 0.65 to 0.95, which is consistent with the simulation results in Fig. 7(b). And the inverter can operate normally under the condition that modulation index changes. The spectra of u_{AN} at $m_a = 0.65,0.95$ are also shown in Fig. 13. The main harmonics of u_{AN} are at the sidebands of 8 kHz, which shows good agreement with the FFT results in Fig. 8(b).

The output power of the cascaded cells is illustrated in Figs. 14 and 15 under PBIH-PWM strategy. Figs. 14 and 15 depict the average output power waveforms of cells H1, H2, H3 with an *R-L* load (20 Ω-4 mH) at $m_a = 0.65, 0.95$, respectively. And the average output power of cascaded cells is measured by a digital power meter. The average output power of cells H1, H2, H3 is 131.63 W, 65.8 W, 65.81 W, respectively, at $m_a = 0.65$. When modulation index is 0.95, the average output power of cells H1, H2, H3 is 279.47 W, 139.5 W, 139.5 W. The ratio of the average output power of cascaded cells is 2.005:1:1 and 2.003:1:1, respectively, at $m_a = 0.65, 0.95$, which presents the 2:1:1 linear relationship. In other words, PBIH-PWM can achieve a balanced power distribution among cascaded cells under different modulation indexes.

Fig. 16 depicts the waveform of the inverter with the changes of load from RL_1 (50 Ω-4 mH, PF = 0.99) to R_1 (50 Ω, PF = 1) and from R_1 (50 Ω, PF = 1) to R_2L_2 (50 Ω-30 mH, PF = 0.98) at $m_a = 0.65$. Despite abrupt load changes, the inverter output voltage is still a nine-level PWM waveform. The inverter performance is excellent when load changes.

The thermal pictures of the switching devices of cells H2, H3 at $m_a = 0.65, 0.95$ are shown in Fig. 17. As can be seen,

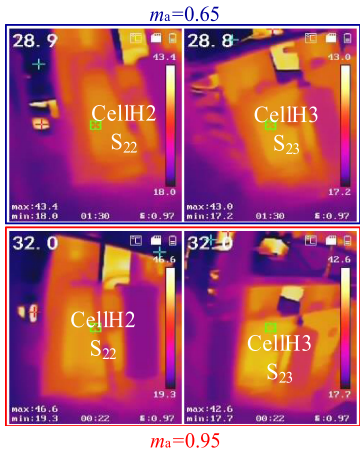

Fig. 17. Thermal pictures of devices under different modulation indexes.

the temperature of the switching devices S_{22} and S_{23} are the same under different modulation indexes. Thus, the PBIH-PWM strategy can balance the switching loss of the low-voltage cells effectively.

The experiment results show that the PBIH-PWM strategy can achieve a balanced power distribution among cascaded cells and balance the loss of devices among cells H2, H3. In addition, the PBIH-PWM strategy has good dynamic performance under changes in modulation index and load.

IX. Conclusion

A PBIH-PWM strategy is proposed in this article, which can achieve a balanced power distribution among cascaded cells of ACHBMLIs with an asymmetric ratio of 2:1:1. The scheme is founded on modifying the conducting angle of cell H1 and alternating the carriers of cells H2, H3. And the extensive simulation and experiment results show the following.

1) Under the full modulation indexes, the average output power of cell H1 increases linearly from 0 to $EI\cos\varphi$, and the average output power of cells H2, H3 increases linearly from 0 to 0.5 $EI\cos\varphi$. The ratio of the average output power of cascaded cells is always 2:1:1. Besides, the switching loss of cells H2, H3 is uniform under different modulation indexes.
2) The scheme has good dynamic performance: the inverter output voltage varies from a PWM wave of 5-level to 7-level output, then to 9-level with the change in modulation index from 0.35 to 0.65, and then to 0.95. And the output voltage u_{AN} maintains normal despite sudden load change. The THD of inverter output current i_{o} is lower than 3% with resistance-inductance load.
3) A generalized scheme based on PBIH-PWM strategy is presented in appendix, which is designed for ACHBMLIs with an asymmetric ratio i:1:1:1. . . .. Only by modifying the conducting angel of high-voltage cell to satisfy the relation $\alpha = \mathrm{acos}(\pi m_{\mathrm{a}}/4)$ and rotating the carriers of low-voltage cells, the targets of power balance among cascaded cells and uniform switching loss of low-voltage cells can be achieved.

Appendix

This article presents a scheme for ACHBMLIs with an asymmetric ratio of 2:1:1, which can achieve a linearly balanced power distribution among cascaded cells and uniform switching loss of cells H2, H3. The scheme can be extended to ensure the cascaded cells of ACHBMLIs operate at a balanced power regime, whose asymmetric ratio is i:1:1:1 . . . .. When the conducting angle of the high voltage cell satisfies the relation $\alpha = \mathrm{acos}(\pi m_{\mathrm{a}}/4)$ and carriers are rotated, the targets of power balance among cascaded cells and uniform switching loss of low-voltage cells can be achieved.

Taking ACHBLIs with an asymmetric ratio of 2:1:1:1 as an example, the corresponding modulation strategy principle is shown in Fig. 18(a). When the conducting angle of cell H1 satisfies the relation $\alpha = \mathrm{acos}(\pi m_{\mathrm{a}}/4)$, the amplitude of fundamental component of cell H1 can be expressed as follows:

$$u_{\mathrm{H1}(1)} = \frac{8E}{\pi}\cos(\mathrm{acos}(\pi m_{\mathrm{a}}/4)) = 2m_{\mathrm{a}}E. \tag{25}$$

And after carrier rotation, the fundamental amplitude of the output voltage of the low-voltage cells can be calculated as follows:

$$u_{\mathrm{H2}(1)} = u_{\mathrm{H3}(1)} = u_{\mathrm{H4}(1)} = \frac{1}{3}(5m_{\mathrm{a}}E - u_{\mathrm{H1}(1)}) = m_{\mathrm{a}}E. \tag{26}$$

The average output power of cascaded cells can be obtained as follows:

$$P_{\mathrm{H1}} = m_{\mathrm{a}}EI\cos\varphi, P_{\mathrm{H2}} = P_{\mathrm{H3}} = P_{\mathrm{H4}} = 0.5m_{\mathrm{a}}EI\cos\varphi. \tag{27}$$

According to the previous switching loss analysis, the switching loss among cells H2, H3, H4 is uniform.

Similarly, when the scheme is applied to ACHBMLIs with an asymmetric ratio of 3:1:1:1, whose principle is depicted in Fig. 18(b), the amplitude of fundamental component of cell H1 can be expressed as follows:

$$u_{\mathrm{H1}(1)} = \frac{12E}{\pi}\cos(\mathrm{acos}(\pi m_{\mathrm{a}}/4)) = 3m_{\mathrm{a}}E. \tag{28}$$

And the fundamental amplitude of the output voltage of cells H2, H3, H4 can be calculated as follows:

$$u_{\mathrm{H2}(1)} = u_{\mathrm{H3}(1)} = u_{\mathrm{H4}(1)} = \frac{1}{3}(6m_{\mathrm{a}}E - u_{\mathrm{H1}(1)}) = m_{\mathrm{a}}E. \tag{29}$$

The average output power of cascaded cells can be obtained as follows:

$$P_{\mathrm{H1}} = 1.5m_{\mathrm{a}}EI\cos\varphi, P_{\mathrm{H2}} = P_{\mathrm{H3}} = P_{\mathrm{H4}} = 0.5m_{\mathrm{a}}EI\cos\varphi. \tag{30}$$

And the switching loss among cells H2, H3, H4 is uniform.

Fig. 19 shows the relationship between the cascaded cell's average output power and the modulation index above-mentioned two ACHBMLIs. It can be seen from Fig. 19(a): when modulation index $m_{\mathrm{a}} \in [0,1]$, the average output power of cell H1 increases linearly from 0 to $EI\cos\varphi$, and the average output power of cells H2, H3, H4 increases linearly from 0 to $0.5EI\cos\varphi$. As can be observed in Fig. 19(b), the average output power of cascaded cells increases linearly, respectively, and balanced power

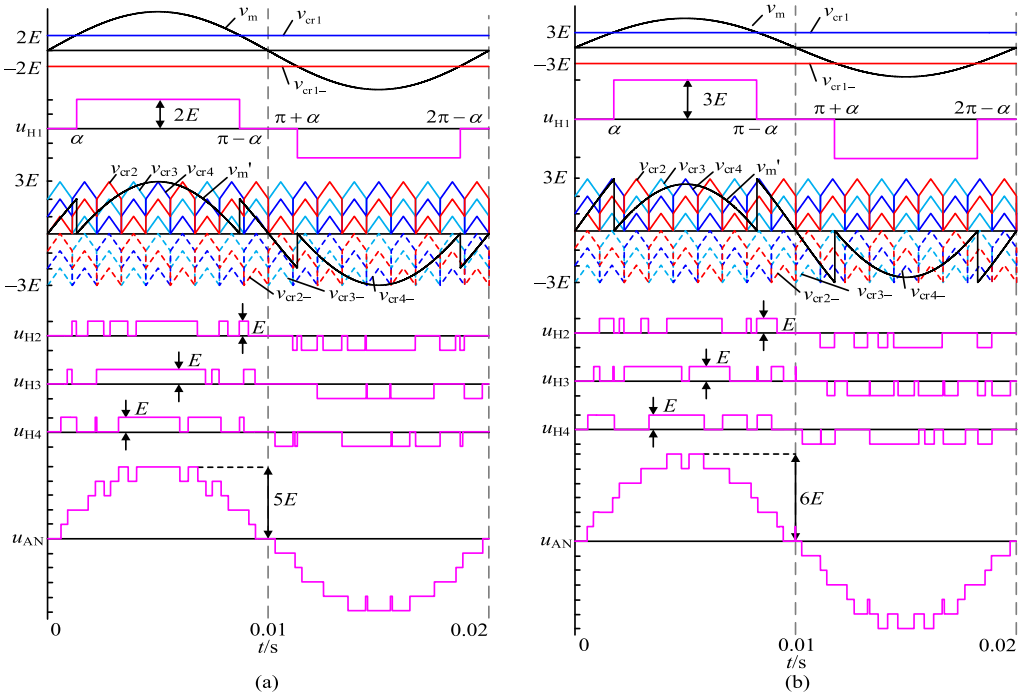

Fig. 18. Principle of the generalized scheme. (a) 2:1:1:1 ACHBMLIs. (b) 3:1:1:1 ACHBMLIs.

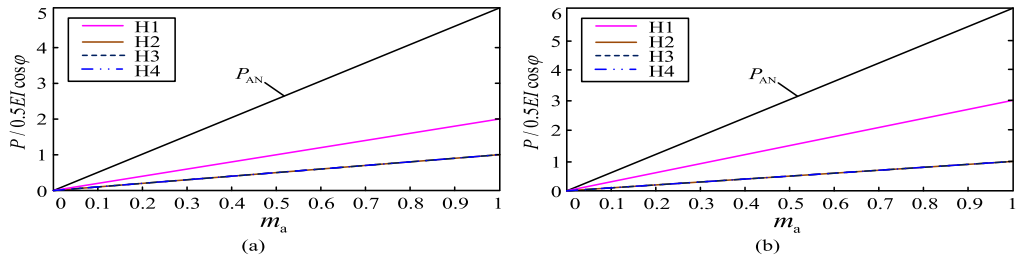

Fig. 19. Relationship between the cascaded cells' average output power and the modulation index under the generalized scheme (a). 2:1:1:1 ACHBMLIs. (b) 3:1:1:1 ACHBMLIs.

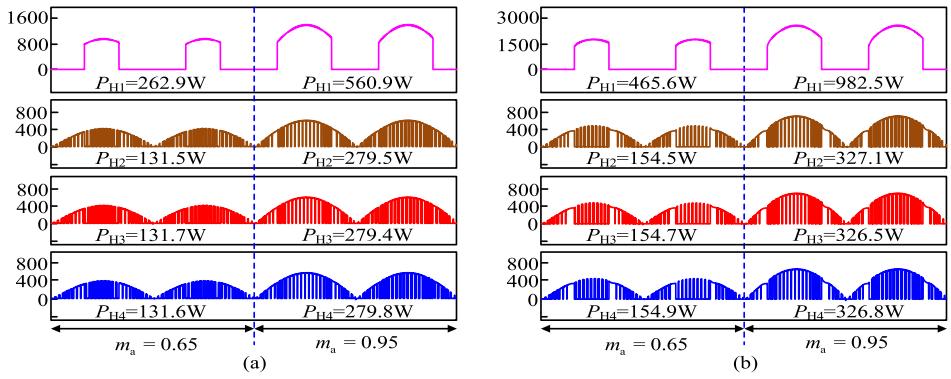

Fig. 20. Simulation results under the generalized scheme. (a) 2:1:1:1 ACHBMLIs. (b) 3:1:1:1 ACHBMLIs.

distribution among cascaded cells is achieved under the full modulation indexes. Simulation results are presented in Fig. 20 when the scheme is applied to the ACHBMLIs with an asymmetric ratio of 2:1:1:1 and 3:1:1:1. The ratio of the average output power of cascaded cells is very close to 2:1:1:1 and 3:1:1:1 at m_a = 0.65, 0.95, respectively. In other words, power balance among cascaded cells is achieved. Hence, the scheme can be applied to ACHBMLIs with an asymmetric ratio of i:1:1:1 . . . . , which can achieve a balanced power distribution among cascaded cells and uniform switching loss among low-voltage cells.

However, the scheme has some drawbacks: the number of the rotated carriers increases when the number of cascaded cells increases, which increases the complexity of digital implementation. But this drawback can be overcome by the controller based on DSP cooperates with FPGA to implement the proposed scheme. In addition, when the scheme is applied to ACHBMLIs with an asymmetric ratio of i: i … 1:1:1:1 …, it can only achieve a balanced power distribution among all cascaded cells under partial modulation indexes.

REFERENCES

[1] A. Salem, H. V. Khang, K. G. Robbersmyr, M. Norambuena, and J. Rodriguez, "Voltage source multilevel inverters with reduced device count: Topological review and novel comparative factors," *IEEE Trans. Power Electron.*, vol. 36, no. 3, pp. 2720–2747, Mar. 2021.

[2] P. R. Bana, K. P. Panda, and G. Panda, "Power quality performance evaluation of multilevel inverter with reduced switching devices and minimum standing voltage," *IEEE Trans. Ind. Inform.*, vol. 16, no. 8, pp. 5009–5022, Apr. 2020.

[3] P. Kala and S. Arora, "A comprehensive study of classical and hybrid multilevel inverter topologies for renewable energy applications," *Renewable Sustain. Energy Rev.*, vol. 76, pp. 905–931, Sep. 2017.

[4] S. K. Chattopadhyay and C. Chakraborty, "Full-bridge converter with naturally balanced modular cascaded H-bridge waveshapers for offshore HVDC transmission," *IEEE Trans. Sustain. Energy*, vol. 11, no. 1, pp. 271–281, Jan. 2020.

[5] N. M. Cm, K. V., S. S. Kurmar, and P. Jayaprakash, "An improved H-bridge multilevel inverter-based multi-objective photovoltaic power conversion system," *IEEE Trans Ind. Appl*, to be published, doi: 10.1109/TIA.2021.3101465.

[6] K. K. Gupta, A. Ranjan, P. Bhatnagar, L. K. Sahu, and S. Jain, "Multilevel inverter topologies with reduced device count: A review," *IEEE Trans. Power Electron.*, vol. 31, no. 1, pp. 135–151, Jan. 2016.

[7] H. R. Massrur, T. Niknam, M. Mardaneh, and A. H. Rajaei, "Harmonic elimination in multilevel inverters under unbalanced voltages and switching deviation using a new stochastic strategy," *IEEE Trans. Ind. Inform.*, vol. 12, no. 2, pp. 716–725, Apr. 2016.

[8] M. Malinowski, K. Gopakumar, J. Rodriguez, and M. A. Peérez, "A survey on cascaded multilevel inverters," *IEEE Trans. Ind. Electron.*, vol. 57, no. 7, pp. 2197–2206, Jul. 2010.

[9] X. Guo *et al.*, "Leakage current suppression of three-phase flying capacitor PV inverter with new carrier modulation and logic function," *IEEE Trans. Power Electron.*, vol. 33, no. 3, pp. 2127–2135, Mar. 2018.

[10] R. Vasu, S. K. Chattopadhyay, and C. Chakraborty, "Asymmetric cascaded h-bridge multilevel inverter with single dc source per phase," *IEEE Trans. Ind. Electron.*, vol. 67, no. 7, pp. 5398–5409, Jul. 2020.

[11] E. Samadaei, S. A. Gholamian, A. Sheikholeslami, and J. Adabi, "An envelope type (E-type) module: Asymmetric multilevel inverters with reduced components," *IEEE Trans. Ind. Electron.*, vol. 63, no. 11, pp. 7148–7156, Nov. 2016.

[12] E. Babaei and M. S. Moeinian, "Asymmetric cascaded multilevel inverter with charge balance control of a low resolution symmetric subsystem," *Energy Convers. Manage.*, vol. 51, no. 11, pp. 2272–2278, 2010.

[13] R. Lei., C. Gong, K. He, and Z. Yao, "A modified hybrid modulation scheme with even switch thermal distribution for h-bridge hybrid cascaded inverters," *IET Power Electron.*, vol. 10, no. 2, pp. 261–268, Feb. 2016.

[14] P. R. Javier, B. J. Jose A., H. L. Jesús H., and U. R. Francisco R., "Hybrid modulation strategy for asymmetrical cascade h-bridge multilevel inverters," *IEEE Latin Amer. Trans.*, vol. 16, no. 6, pp. 1623–1630, Jun. 2018.

[15] D. Ronanki and S. S. Williamson, "Voltage ripple minimization in modular multilevel converters using modified rotative PWM scheme," in *Proc. AEIT Int. Annu. Conf.*, 2018, pp. 1–6.

[16] I. Sarkar and B. G. Fernandes, "Modified hybrid multi-carrier PWM technique for cascaded H-Bridge multilevel inverter," in *Proc. 40th Annu. Conf. IEEE Ind. Electron. Soc.*, 2014, pp. 4318–4324.

[17] C. I. Odeh, A. Lewicki, and M. Morawiec, "A single-carrier-based pulse-width modulation template for cascaded H-bridge multilevel inverters," *IEEE Access*, vol. 9, pp. 42182–42191, 2021.

[18] O. Lopez-Santos, C. A. Jacanamejoy-Jamioy, D. F. Salazar-D'Antonio, J. R. Corredor-Ramírez, G. Garcia, and L. Martinez-Salamero, "A single-phase transformer-based cascaded asymmetric multilevel inverter with balanced power distribution," *IEEE Access*, vol. 7, pp. 98182–98196, 2019.

[19] M. Ye, L. Kang, Y. Xiao, P. Song, and S. Li, "Modified hybrid modulation strategy with power balance control for H-bridge hybrid cascaded seven-level inverter," *IET Power Electron.*, vol. 11, no. 6, pp. 1046–1054, May 2018.

[20] M. Ye, Q. Wei, W. Ren, and G. Song, "Modified modulation strategy of 1: 1: 2 asymmetric nine-level inverter and its power balance method," *Electronics*, vol. 9, no. 1, pp. 75, Jan. 2020.

[21] Fairchild Semiconductor GmbH, SGH40N60UFD product specification sheet, South Portland, America, 2003.

[22] A. D. Rajapakse, A. M. Gole, and P. L. Wilson, "Electromagnetic transients simulation models for accurate representation of switching losses and thermal performance in power electronic systems," *IEEE Trans. Power Del.*, vol. 20, no. 1, pp. 319–327, Jan. 2005.

Manyuan Ye (Member, IEEE) received the Ph.D. degree in traffic control and information engineering from East China Jiaotong University (ECJTU), Nanchang, China.

He is currently a Professor and Doctoral Supervisor with the School of Electrical and Automation Engineering, ECJTU. His research interests include power electronics and electric drives, modular multilevel converter, pulsewidth modulation, and selective harmonic elimination techniques.

Ruifan Peng received the B.S. degree in electrical engineering in 2019 from East China Jiaotong University, Nanchang, China, where he is currently working toward the M.S. degree in electrical engineering.

His current research interests include power electronics and cascaded multilevel converter.

Ziwei Tong received the B.S. degree in electrical engineering from the Chengdu University of Information Technology, Chengdu, China, in 2019. He is currently working toward the M.S. degree with East China Jiaotong University, Nanchang, China.

His research interests include power electronics and cascaded multilevel converter.

Zihao Chen received the B.S. degree in electrical engineering in 2018 from East China Jiaotong University, Nanchang, China, where he is currently working toward the M.S. degree.

His research interests include power electronics and cascaded multilevel converter.

Zhilin Miao received the B.S. degree in electrical engineering from the Shandong University of Science and Technology, Shandong, China, in 2019. He is currently working toward the M.S. degree with East China Jiaotong University, Nanchang, China.

His research interests include power electronics and cascaded multilevel converter.